

# Flexible and Iridescent Chiral Nematic Mesoporous Organosilica Films

Kevin E. Shopsowitz,<sup>†</sup> Wadood Y. Hamad,<sup>‡</sup> and Mark J. MacLachlan<sup>\*,†</sup>

<sup>†</sup>Department of Chemistry, University of British Columbia, 2036 Main Mall, Vancouver, British Columbia, Canada V6T 1Z1

<sup>‡</sup>FP Innovations, 3800 Wesbrook Mall, Vancouver, British Columbia, Canada V6S 2L9

**S** Supporting Information

**ABSTRACT:** Nanocrystalline cellulose (NCC) has been used to template ethylene-bridged mesoporous organosilica films with long-range chirality and photonic properties. The structural color of the organosilica films results from their chiral nematic ordering, can be varied across the entire visible spectrum, and responds to the presence of chemicals within the mesopores. To synthesize these materials, acid hydrolysis was used to remove the NCC template without disrupting the organosilica framework. The resulting mesoporous organosilica films are much more flexible than brittle mesoporous silica films templated by NCC. These materials are the first of a novel family of chiral mesoporous organosilicas with photonic properties.

Lytotropic liquid crystal templating is a versatile tool for synthesizing materials with periodic nanostructures. The prototypical example of this approach is the use of surfactants to template mesoporous silica (e.g., MCM-41, SBA-15), giving access to solids with well-ordered pore structures that are easily modified based on the template and conditions employed.<sup>1,2</sup> The incorporation of organic functionality into mesoporous silicas provides a way to further fine tune their properties. An important advance in this area took place with the discovery that by using bridged silsesquioxane precursors of the type  $R(\text{Si}(\text{OR})_3)_2$ , periodic mesoporous organosilicas (PMOs) with integral organic groups could be directly synthesized using liquid crystal templating.<sup>3–10</sup> The direct use of bridged organosilica precursors provides a distinct advantage compared to postsynthetic grafting by allowing precise stoichiometric control over the relative amounts of inorganic and organic components within the hybrid material.<sup>11</sup> Also, by incorporating the organic groups as integral components of the cross-linked structure, it is possible to not only change the chemical environment within the pores but also to modify material properties, such as mechanical strength, hydrothermal stability, and molecular organization.<sup>12–14</sup>

PMOs have been synthesized with diverse organic components providing potential applications in many areas, including catalysis, chromatography, sensors, insulating materials, and fuel cells.<sup>15–25</sup> PMOs incorporating chiral bridging groups have been synthesized and proven to be effective materials for enantioselective catalysis and separation.<sup>26–32</sup> Another approach to generate chiral PMOs is to use a chiral template.<sup>33</sup> The use of abundant, naturally occurring chiral

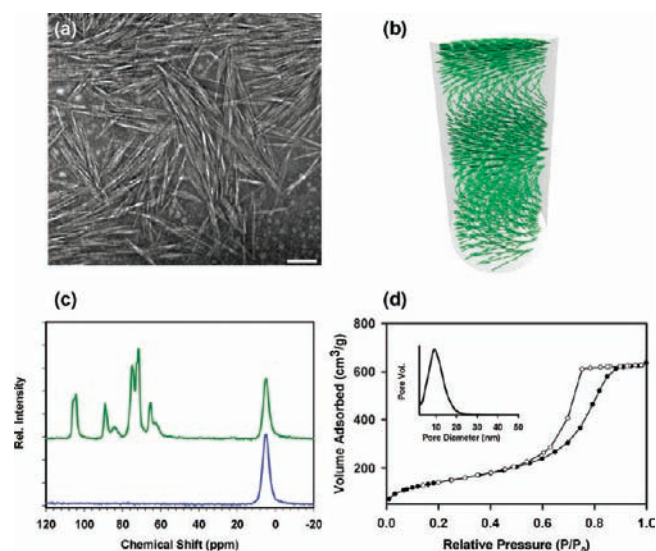


**Figure 1.** (a) TEM image of negatively stained NCC dropcast from a dilute suspension (scale bar = 200 nm). (b) Schematic illustration of the chiral nematic organization of NCC embedded within an organosilica matrix. (c) Solid-state <sup>13</sup>C CP/MAS NMR spectra of composite sample C3 (green) and mesoporous organosilica CMO3 (blue). (d) N<sub>2</sub> isotherm and BJH pore-size distribution (inset) for CMO3.

polymers as templates provides an attractive route to generate enantiopure mesoporous organosilica materials. Along with the possibility of chiral imprinting into the mesopores of the organosilica, which could be useful for enantioselective recognition and separation, biological polymers can also template long-range, chiral photonic structures into mesoporous materials.<sup>34,35</sup> The strong dependence of the selective reflection signal of mesoporous photonic crystals on changes in refractive index has been exploited for the detection of organic vapors and even different bacterial strains.<sup>35–38</sup>

Cellulose is the main structural component of plants and, being comprised entirely of D-glucose monomers, is inherently chiral. Bulk cellulose may be converted into spindle-shaped nanocrystalline cellulose (NCC, Figure 1a) that behaves as a chiral nematic lyotropic liquid crystal.<sup>39–41</sup> We recently demonstrated that NCC may be used to template brittle mesoporous silica and carbon films with left-handed helical

Received: November 3, 2011

Published: December 21, 2011

structures.<sup>35,42</sup> Here we report the synthesis of flexible mesoporous organosilica films that selectively reflect left-handed circularly polarized light. To the best of our knowledge, this is the first example of a mesoporous organosilica film with a periodic photonic structure. The photonic properties of the films come from the chiral nematic structure imparted by the NCC template (Figure 1b), while their flexibility is due to the unique mechanical properties of bridged organosilicas.<sup>43</sup> We expect that the materials reported herein will be the first of a new family of functional photonic materials based on organosilica chemistry. The combination of a chiral, mesoporous photonic structure with the versatility of organosilica chemistry opens the door for new tunable materials that could find use in optical sensing devices and enantioselective separation.

NCC suspensions produced through sulfuric acid hydrolysis of wood pulp<sup>44</sup> were used in this study as the chiral nematic liquid crystal template, while 1,2-bis(trimethoxysilyl)ethane (BTMSE) and 1,2-bis(triethoxysilyl)ethane (BTSE) were initially used as the organosilica precursors. When we set out, we were uncertain whether the organosilica precursors would be compatible with the chiral nematic self-assembly of NCC and whether it would be possible to remove NCC from the composite materials without degrading the organic bridging groups. BTMSE and BTSE were first tested for their ability to form homogeneous mixtures with NCC without disrupting its chiral nematic self-assembly. When added to isotropic NCC suspensions (3 wt % in water, pH 2.4), both organosilica precursors were initially immiscible. The trimethoxysilyl precursor became miscible after stirring for several minutes at room temperature but several hours at over 60 °C were required to achieve a homogeneous mixture with BTSE, owing to the slower rate of hydrolysis for the ethoxy precursor. We therefore focused on BTMSE for the remainder of our experiments. After stirring for 1 h at 20 °C, the mixtures of NCC and BTMSE were allowed to dry in polystyrene Petri dishes under ambient conditions to obtain free-standing films. The composite films show strong selective reflection of light, demonstrating that BTMSE does not negatively affect the self-assembly of NCC into a chiral nematic structure. We see a red shift in the reflectance peaks of the NCC-organosilica composite films with increasing amounts of BTMSE, allowing the optical properties of the films to be easily tuned. This red shift may be caused by an increase in the thickness of the organosilica walls with increasing BTMSE and modulation of the electrostatic interactions between the sulfate groups of NCC. By varying the relative amounts of BTMSE and NCC, four different composite samples were obtained with reflectance peaks ranging from 700 to 900 nm (C1–C4 in order of increasing BTMSE loading, see the Supporting Information, Figure S1). Figure 1b depicts the chiral nematic organization of the NCC within the organosilica matrix.

A novel approach had to be developed to remove NCC from the composite materials and generate mesoporous organosilica since high-temperature calcination led to decomposition of the organosilica. We found that selective decomposition and removal of cellulose from the NCC-organosilica composites could be accomplished by heating the films to 100 °C in 6 M sulfuric acid. This treatment gave films with a slightly brown color due to the presence of insoluble cellulosic byproducts. These byproducts were eliminated by a brief rinse with a H<sub>2</sub>O<sub>2</sub>/H<sub>2</sub>SO<sub>4</sub> solution to give transparent and completely colorless films that became strongly iridescent after drying. The

films remained intact for the most part during the cellulose removal procedure, and we obtained free-standing organosilica films with dimensions of several centimeters (Figure 2a). Four mesoporous organosilica samples were prepared (CMO1–CMO4) from composite samples C1–C4, respectively.

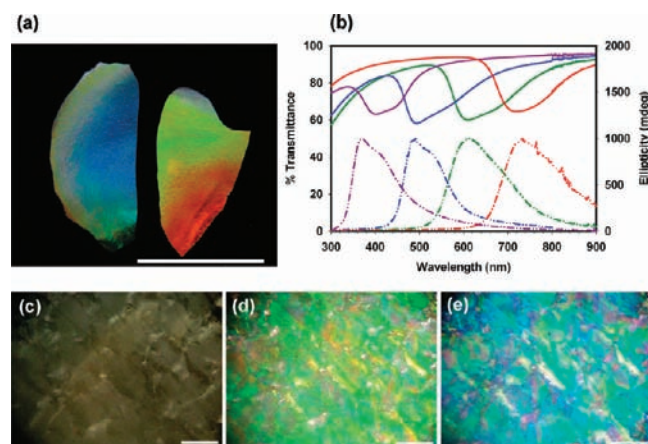


**Figure 2.** Optical characterization of mesoporous organosilica films. (a) Photograph showing samples CMO2 and CMO3 (scale bar = 18 mm). (b) UV-vis transmittance spectra (solid curves) and CD spectra (dashed curves) of CMO1 (purple), CMO2 (blue), CMO3 (green), and CMO4 (red). (c–e) POM micrographs of CMO2 at different time points following soaking with acetone (scale bars = 200  $\mu$ m).

The complete removal of NCC and retention of the ethylene bridge in the organosilica films were confirmed using a variety of techniques. Solid-state <sup>13</sup>C and <sup>29</sup>Si cross-polarization magic-angle spinning (CP/MAS) NMR spectroscopy was carried out before and after the acid hydrolysis procedure. The <sup>13</sup>C NMR spectrum of the composite material shows peaks between 60 and 120 ppm assigned to cellulose and a single peak at 5 ppm that corresponds to the ethylene (SiCH<sub>2</sub>CH<sub>2</sub>Si) carbons of the organosilica (Figure 1c).<sup>3,4</sup> After the acid hydrolysis treatment, only the single peak of the organosilica remains, demonstrating that cellulose was successfully removed. Solid-state <sup>29</sup>Si CP/MAS NMR, both before and after NCC removal, shows peaks characteristic of ethylene-bridged organosilica at –65 and –57 ppm that can be assigned to T<sup>3</sup> (CSi(OSi)<sub>3</sub>) and T<sup>2</sup> (CSi(OSi)<sub>2</sub>OH) Si atoms, respectively (Figure S2, Supporting Information).<sup>3,4</sup> The absence of signals corresponding to SiO<sub>4</sub> species between –90 and –120 ppm demonstrates that Si–C bond cleavage does not occur during NCC removal. Elemental analysis of the organosilica samples shows that they contain 14 wt % carbon and 4 wt % hydrogen. These results suggest an ethylene-bridged organosilica material with an estimated formula of C<sub>2</sub>H<sub>7</sub>Si<sub>2</sub>O<sub>4.5</sub>, implying a considerable amount of uncondensed Si–OH groups, consistent with the intensity of the T<sup>2</sup> peak in the <sup>29</sup>Si NMR spectrum. Thermogravimetric analysis (TGA) shows that the organosilica is stable up to 400 °C, after which decomposition of 14–18 wt % occurs (Figure S3b, Supporting Information). In contrast, elemental analysis and TGA of mesoporous silica control samples that were prepared using the same procedure (except with Si(OCH<sub>3</sub>)<sub>4</sub> used in place of BTMSE) show that no residual organic material is present (Figure S3c, Supporting Information), further confirming that the acid hydrolysis conditions employed are sufficient for the complete degradation and removal of cellulose.

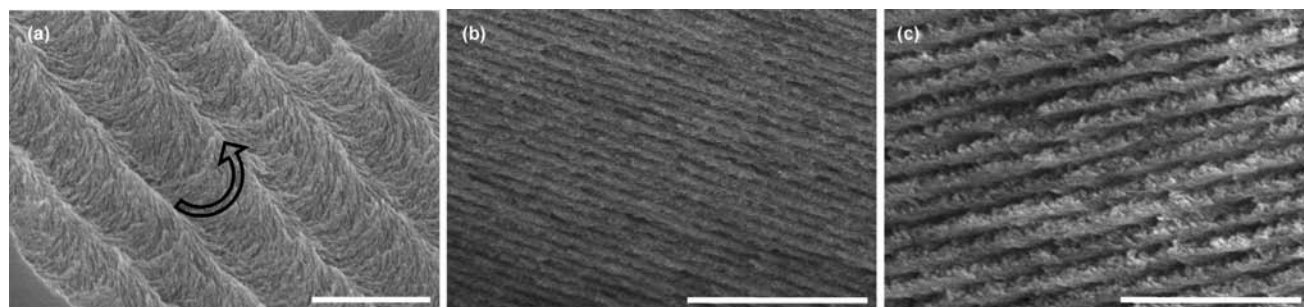


**Figure 3.** SEM images of chiral nematic mesoporous silica. (a) Cross-sectional view at high magnification of CMO3 reveals a left-handed chiral nematic structure (scale bar = 1  $\mu\text{m}$ ). The arrow indicates a 180° counter-clockwise rotation of the director, i.e., one-half helical pitch. (b) Cross-section of CMO1 reveals long-range ordering with an average helical pitch of 290 nm (scale bar = 2  $\mu\text{m}$ ). (c) Cross-section of CMO4 reveals long-range ordering with an average helical pitch of 510 nm (scale bar = 2  $\mu\text{m}$ ).

The ethylene-bridged mesoporous organosilica films show significantly improved mechanical properties compared to pure mesoporous silica (either prepared by calcination or acid treatment of NCC-silica composites). Whereas the pure silica films are very brittle, the organosilica films are considerably less fragile and are fairly flexible (see video, Supporting Information). Large crack-free films can be readily prepared that can be handled with tweezers, bent, and easily attached to different substrates. Due to their flexibility, when the mesoporous organosilica films absorb liquids, they rapidly flex toward the direction of the liquid before relaxing again.

Tensile strength measurements were conducted on free-standing films of mesoporous organosilica and silica (prepared by acid hydrolysis of an NCC-silica composite). Stress–strain curves confirm that the organosilica films are less brittle than their silica counterparts and can withstand greater stress and strain before fracturing (Figure S4, Supporting Information). The improved mechanical properties of ethylene-bridged mesoporous organosilica films were recently attributed to bond trapping phenomena that lead to superior fracture energies.<sup>43</sup>

Porosity of the organosilica films was investigated using nitrogen adsorption–desorption (Figure 1d). The organosilica samples display type IV isotherms with significant hysteresis, which is indicative of mesoporosity. BET surface areas and specific pore volumes ranging from 400 to 500  $\text{m}^2/\text{g}$  and 0.6–1  $\text{cm}^3/\text{g}$ , respectively, were calculated for samples CMO1–CMO4. The Barrett, Joyner, and Halenda model (BJH) pore size distributions of the mesoporous organosilica are broad with peaks typically between 8 and 9 nm (Figure 1d), which is considerably larger than the 3–4 nm pores obtained for NCC-templated mesoporous silica generated by calcination.<sup>35</sup> The reason for the larger pore diameter of the organosilica films may simply be that the use of acid hydrolysis to remove NCC avoids the significant contraction that occurs during calcination. This is supported by transmission electron microscopy (TEM) of the NCC template, which reveals diameters ranging from ~5–15 nm, suggesting that the pore size distribution of the organosilica more closely reflects the diameter range of the NCC template compared to the calcined silica.

Organosilica samples CMO1–CMO4 have peak reflectance wavelengths that cover the visible spectrum from 400 to 750 nm (Figure 2b). The iridescence of the mesoporous organosilica films indicates that their chiral nematic structure is retained after NCC removal. This was further confirmed by circular dichroism (CD), which shows strong positive signals with positions that match up closely with the reflectance peaks

of the films, indicating that they selectively reflect left-handed circularly polarized light (Figure 2b, note that due to the extremely large CD signal generated by these materials, small pieces of film were used to avoid saturating the detector). The colors of the organosilica films were all blue-shifted relative to the corresponding composite films. Selective reflection from a chiral nematic structure for normal incident light follows the following equation:

$$\lambda_{\text{max}} = n_{\text{avg}}P \quad (1)$$

where  $n_{\text{avg}}$  is the average refractive index and  $P$  is the helical pitch. A blue shift of the reflectance peak can therefore be caused by a decrease in either of these two variables. In the case of the organosilica films, we find that the blue shift is mostly attributed to the decrease in refractive index that occurs upon the removal of NCC. This is in contrast to the calcined mesoporous silica films, which also show a substantial decrease in helical pitch upon NCC removal.<sup>35</sup>

Absorption of liquids into the chiral nematic organosilica films causes a reversible loss of iridescence due to refractive index matching between the pores and walls of the material (see video, Supporting Information). Observing a film soaked in acetone as it dried using POM, we could see it rapidly regain birefringence as the bulk of the liquid evaporated from the mesopores (Figure 2c,d). The film then gradually changed back to its original color as the remaining adsorbed acetone evaporated (Figure 2d,e). CD spectra were also measured for the organosilica films after soaking with different liquids (Figure S5, Supporting Information). The CD spectra of the wet films show dramatically reduced intensities compared to the dry films. Because the refractive indices of the liquids used do not match perfectly with that of the organosilica walls, reflection still occurs from the wet films that, although undetectable to the naked eye, produces a CD signal. The intensity of the CD signal strongly depends on the refractive index of the liquid absorbed into the films. For example, DMSO ( $n = 1.48$ ) causes a much larger decrease in CD signal compared to water ( $n = 1.33$ ).

The chiral nematic organization of the mesoporous organosilica films was directly observed by scanning electron microscopy (SEM). At fractures perpendicular to the surface of the films, we observe a rod-like texture with a director that rotates in a counter-clockwise direction (Figure 3a). This gives rise to the long-range helical structure responsible for the selective reflection of light. Looking at cross sections of the films, the periodic structure is present throughout their entire thickness, where each repeating band corresponds to a 180°

rotation of the chiral nematic director (i.e., a half helical pitch). Comparing the SEM cross sections of samples **CMO1** and **CMO4**, it is apparent that the helical pitch of **CMO1** ( $P = 290$  nm, Figure 3b) is considerably shorter than that of **CMO4** ( $P = 510$  nm, Figure 3c). This shows that increasing the relative amount of BTMSE used to synthesize the films causes an increase in their helical pitch, which in turn causes a red shift of their reflected colors.

In conclusion, we have shown that NCC can be used to template free-standing films of ethylene-bridged mesoporous organosilica with a chiral nematic structure. This approach should be expandable to other organosilica precursors of the type  $(\text{MeO})_3\text{SiRSi}(\text{OMe})_3$ . In the current study, the incorporation of an ethylene bridge into the mesoporous organosilica films results in improved mechanical properties and flexibility compared to pure silica. Future work incorporating other organic groups into these materials should provide a means to generate mesoporous films with highly tunable optical properties, mechanical properties, and chemical selectivity. These materials could have potential applications in optical devices, sensors, and chiral separation.

## ■ ASSOCIATED CONTENT

### ■ Supporting Information

Additional experimental details and figures as well as videos demonstrating the flexibility, solvent adsorption, and circular polarized iridescence of the mesoporous organosilica films. This material is available free of charge via the Internet at <http://pubs.acs.org>.

## ■ AUTHOR INFORMATION

### ■ Corresponding Author

[mmaclach@chem.ubc.ca](mailto:mmaclach@chem.ubc.ca)

## ■ ACKNOWLEDGMENTS

We thank NSERC and FPInnovations for support, NSERC for a graduate fellowship (to K.E.S.), and Prof. Carl Michal and Alan Manning (UBC Physics) for the solid-state NMR data.

## ■ REFERENCES

- (1) Kresge, C. T.; Leonowicz, M. E.; Roth, W. J.; Vartuli, J. C.; Beck, J. S. *Nature* **1992**, *359*, 710–712.
- (2) Yang, P.; Zhao, D.; Margolese, D. I.; Chmelka, B. F.; Stucky, G. D. *Nature* **1998**, *396*, 152–155.
- (3) Inagaki, S.; Guan, S.; Fukushima, Y.; Ohsuna, T.; Terasaki, O. *J. Am. Chem. Soc.* **1999**, *121*, 9611–9614.
- (4) Melde, B. J.; Holland, B. T.; Blanford, C. F.; Stein, A. *Chem. Mater.* **1999**, *11*, 3302–3308.
- (5) Asefa, A.; MacLachlan, M. J.; Coombs, N.; Ozin, G. A. *Nature* **1999**, *402*, 867–871.
- (6) Yoshina-Ishii, C.; Asefa, T.; Coombs, N.; MacLachlan, M. J.; Ozin, G. A. *Chem. Commun.* **1999**, 2539–2540.
- (7) Cho, E. -B.; Kim, D.; Jaroniec, M. *J. Phys. Chem. C* **2008**, *112*, 4897–4902.
- (8) Mizoshita, N.; Ikai, M.; Tani, T.; Inagaki, S. *J. Am. Chem. Soc.* **2009**, *131*, 14225–14227.
- (9) Haffer, S.; Tiemann, M.; Fröba, M. *Chem.—Eur. J.* **2010**, *16*, 10447–10452.
- (10) Wang, W.; Grozea, D.; Kohli, S.; Perovic, D. D.; Ozin, G. A. *ACS Nano* **2011**, *5*, 1267–1275.
- (11) Lim, M. H.; Stein, A. *Chem. Mater.* **1999**, *11*, 3285–3295.
- (12) Lu, Y.; Fan, H.; Doke, N.; Loy, D. A.; Assink, R. A.; LaVan, D. A.; Brinker, C. J. *J. Am. Chem. Soc.* **2000**, *122*, 5258–5261.
- (13) Burleigh, M. C.; Markowitz, M. A.; Jayasundera, S.; Spector, M. S.; Thomas, C. W.; Gaber, B. P. *J. Phys. Chem. B* **2003**, *107*, 12628–12634.
- (14) Inagaki, S.; Guan, S.; Ohsuna, T.; Terasaki, O. *Nature* **2002**, *416*, 304–307.
- (15) Hunks, W. J.; Ozin, G. A. *J. Mater. Chem.* **2005**, *15*, 3716–3724.
- (16) Angelos, S.; Johansson, E.; Stoddart, J. F.; Zink, J. I. *Adv. Funct. Mater.* **2007**, *17*, 2261–2271.
- (17) Wang, W.; Lofgreen, J. E.; Ozin, G. A. *Small* **2010**, *6*, 2634–2642.
- (18) Mizoshita, N.; Tani, T.; Inagaki, S. *Chem. Soc. Rev.* **2011**, *40*, 789–790.
- (19) Asefa, T.; Kruk, M.; MacLachlan, M. J.; Coombs, N.; Grondley, H.; Jaroniec, M.; Ozin, G. A. *J. Am. Chem. Soc.* **2001**, *123*, 8520–8530.
- (20) Zhu, F. -X.; Wang, W.; Li, H. -X. *J. Am. Chem. Soc.* **2011**, *133*, 11632–11640.
- (21) Rebbin, V.; Schmidt, R.; Fröba, M. *Angew. Chem., Int. Ed.* **2006**, *45*, 5210–5214.
- (22) Johnson-White, B.; Zeinali, M.; Shaffer, K. M.; Patterson, C. H.; Charles, P. T.; Markowitz, M. A. *Biosens. Bioelectron.* **2007**, *22*, 1154–1162.
- (23) Du, J.; Cipot-Wechsler, J.; Lobez, J. M.; Loock, H. P.; Crudden, C. M. *Small* **2010**, *6*, 1168–1172.
- (24) Wang, W.; Grozea, D.; Kim, A.; Perovic, D. D.; Ozin, G. A. *Adv. Mater.* **2010**, *22*, 99–102.
- (25) Pereira, F.; Vallé, K.; Belleville, P.; Morin, A.; Lambert, S.; Sanchez, C. *Chem. Mater.* **2008**, *20*, 1710–1718.
- (26) Baleizão, C.; Gigante, B.; Das, D.; Alvaro, M.; Garcia, H.; Corma, A. *Chem. Commun.* **2003**, 1860–1861.
- (27) Ide, A.; Voss, R.; Scholz, G.; Ozin, G. A.; Antonietti, M.; Thomas, A. *Chem. Mater.* **2007**, *19*, 2649–2657.
- (28) Inagaki, S.; Guan, S.; Yang, Q.; Kapoor, M. P.; Shimada, T. *Chem. Commun.* **2008**, 202–204.
- (29) Kuschel, A.; Polarz, S. *J. Am. Chem. Soc.* **2010**, *132*, 6558–6565.
- (30) Zhu, G.; Zhong, H.; Yang, Q.; Li, C. *Microporous Mesoporous Mater.* **2008**, *116*, 36–43.
- (31) Morell, J.; Chatterjee, S.; Klar, P. J.; Mauder, D.; Shenderovich, I.; Hoffmann, F.; Fröba, M. *Chem.—Eur. J.* **2008**, *14*, 5935–5940.
- (32) Wu, X.; Blackburn, T.; Webb, J. D.; Garcia-Bennett, A. E.; Crudden, C. M. *Angew. Chem., Int. Ed.* **2011**, *50*, 8095–8099.
- (33) Liu, X.; Zhuang, W.; Li, B.; Wu, L.; Wang, S.; Li, Y.; Yang, Y. *Chem. Commun.* **2011**, 47, 7215–7217.
- (34) Thomas, A.; Antonietti, M. *Adv. Funct. Mater.* **2003**, *13*, 763–766.
- (35) Shopsowitz, K. E.; Qi, H.; Hamad, W. Y.; MacLachlan, M. J. *Nature* **2010**, *468*, 422–425.
- (36) Lin, V. S. -Y.; Motesharei, K.; Dancil, K. -P. S.; Sailor, M. J.; Ghadiri, M. R. *Science* **1997**, *278*, 840–843.
- (37) Kelly, T. L.; Segal, A. G.; Sailor, M. J. *Nano Lett.* **2011**, *11*, 3169–3173.
- (38) Bonifacio, L. D.; Puzzo, D. P.; Breslav, S.; Willey, B. M.; McGeer, A.; Ozin, G. A. *Adv. Mater.* **2010**, *22*, 1351–1354.
- (39) Revol, J. F.; Bradford, H.; Giasson, J.; Marchessault, R. H.; Gray, D. G. *Int. J. Biol. Macromol.* **1992**, *14*, 170–172.
- (40) Habibi, Y.; Lucia, L. A.; Rojas, O. J. *Chem. Rev.* **2010**, *110*, 3479–3500.
- (41) Klemm, D.; Kramer, F.; Moritz, S.; Lindström, T.; Ankerfors, M.; Gray, D.; Dorris, A. *Angew. Chem., Int. Ed.* **2011**, *50*, 5438–5466.
- (42) Shopsowitz, K. E.; Hamad, W. Y.; MacLachlan, M. J. *Angew. Chem., Int. Ed.* **2011**, *50*, 10991–10995.
- (43) Dubois, G.; Volksen, W.; Magbitang, T.; Miller, R. D.; Gage, D. M.; Dauskardt, R. H. *Adv. Mater.* **2007**, *19*, 3989–3994.
- (44) Hamad, W. Y.; Hu, T. Q. *Can. J. Chem. Eng.* **2010**, *88*, 392–402.